# Stripe order, depinning, and fluctuations in $La_{1.875}Ba_{0.125}CuO_4$ and $La_{1.875}Ba_{0.075}Sr_{0.050}CuO_4$

M. Fujita,* H. Goka, and K. Yamada
*Institute for Materials Research, Tohoku University, Katahira, Sendai 980-8577, Japan*

J. M. Tranquada
*Physics Department, Brookhaven National Laboratory, Upton, New York 11973, USA*

L. P. Regnault
*CEA/Grenoble, Département de Recherche Fondamentale sur la Matiére Condensée, 38054 Grenoble cedex 9, France*
(Received 16 March 2004; revised manuscript received 14 June 2004; published 24 September 2004)

We present a neutron scattering study of stripe correlations measured on a single crystal of $La_{1.875}Ba_{0.125}CuO_4$. Within the low-temperature-tetragonal (LTT) phase, superlattice peaks indicative of spin and charge stripe order are observed below 50 K. For excitation energies $\hbar\omega \leqslant 12$ meV, we have characterized the magnetic excitations that emerge from the incommensurate magnetic superlattice peaks. In the ordered state, these excitations are similar to spin waves. Following these excitations as a function of temperature, we find that there is relatively little change in the **Q**-integrated dynamical spin susceptibility for $\hbar\omega \sim 10$ meV as stripe order disappears and then as the structure transforms from LTT to the low-temperature-orthorhombic phase. The **Q**-integrated signal at lower energies changes more dramatically through these transitions, as it must in a transformation from an ordered to a disordered state. We argue that the continuous evolution through the transitions provides direct evidence that the incommensurate spin excitations in the disordered state are an indicator of dynamical charge stripes. An interesting feature of the thermal evolution is a variation in the incommensurability of the magnetic scattering. Similar behavior is observed in measurements on a single crystal of $La_{1.875}Ba_{0.075}Sr_{0.050}CuO_4$; maps of the scattered intensity in a region centered on the antiferromagnetic wave vector and measured at $\hbar\omega = 4$ meV are well reproduced by a model of disordered stripes with a temperature-dependent mixture of stripe spacings. We discuss the relevance of our results to understanding the magnetic excitations in cuprate superconductors.

DOI: 10.1103/PhysRevB.70.104517 PACS number(s): 74.72.Dn, 74.81.−g, 75.40.Gb, 78.70.Nx

## I. INTRODUCTION

High-$T_c$ superconductivity in lamellar copper oxides arises when a sufficient density of carriers is doped into a parent Mott insulator. Upon doping, Néel order disappears but dynamic antiferromagnetic (AF) spin correlations survive and coexist with the induced superconductivity. Thus, the AF spin fluctuations in a doped $CuO_2$ plane are widely believed to have a fundamental connection with the underlying mechanism of high-$T_c$ superconductivity.[1] Extensive neutron scattering measurements have revealed an intimate relationship between the incommensurate (IC) low-energy spin fluctuations observed in $La_{2-x}Sr_xCuO_4$ (LSCO) (Refs. 2–4) and the superconductivity.[5] On the other hand, the discovery of evidence for cooperative spin and charge order in $La_{1.6-x}Nd_{0.4}Sr_xCuO_4$ (LNSCO) provides a new perspective on the charge distribution within the $CuO_2$ planes;[6] doped charge spatially segregates into stripes that separate antiphase AF domains. Such self-organized states of the strongly correlated electrons result in a variety of interesting phenomena[7–9] and have attracted much attention due to their potential role in the mechanism of high-$T_c$ superconductivity.[10–17]

The physics behind the IC spin fluctuations in LSCO remains controversial. To us, the concept of fluctuating stripes[18,19] provides an appealing explanation of the magnetic fluctuations; however, there is an alternative school of thought that argues for an explanation in terms of Fermi-surface-nesting effects.[20–26] This controversy is tied to the issue of whether charge stripe order is incompatible with superconductivity. It is clear experimentally that static ordering of charge stripes is correlated with a depression of $T_c$,[27,28] but are the excitations of the stripe-ordered state different in nature from those in a state without static stripe order?

To address these issues, we present a neutron scattering study of $La_{2-x}Ba_xCuO_4$ (LBCO) with $x = \frac{1}{8}$. This is the material in which high-temperature superconductivity was first discovered[29] and in which the anomalous suppression of $T_c$ at $x = \frac{1}{8}$ was first observed.[30–33] The difference between the Ba- and Sr-doped systems is associated with a subtle transition from the usual low-temperature-orthorhombic (LTO) structure of LSCO to the low-temperature-tetragonal (LTT) phase in the Ba-doped material.[34] The connection between the structural transition and the appearance of charge and spin stripe order has been clearly demonstrated in the $\frac{1}{8}$-doped $La_{1.875}Ba_{0.125-x}Sr_xCuO_4$ (LBSCO) system;[35] however, up until now, the occurrence of stripe order in pure LBCO has not been confirmed due to the difficulty of growing a crystal at the $x = \frac{1}{8}$ composition.[36,37]

We begin our paper by presenting neutron diffraction evidence for stripe order within the LTT phase of $La_{1.875}Ba_{0.125}CuO_4$, obtained using a large single crystal grown at Kyoto University. On cooling, the transition to the LTT phase begins at $T_{d2} = 60$ K, and the magnetic and charge order superlattice peaks appear essentially simultaneously at

 

$T_{st}$=50 K. We then turn to the central topic, which is an investigation of the spin fluctuations for excitation energies in the range $2 \leqslant \hbar\omega \leqslant 12$ meV. We show that these low-energy excitations, which have some characteristics of spin waves within the stripe-ordered phase,[18,39–44] evolve continuously through the LTT-to-LTO transition. For $\hbar\omega \sim 10$ meV, there is relatively little change in the imaginary part of the dynamic spin susceptibility $\chi''(\mathbf{Q},\omega)$ through the transition, while at lower energies the **Q**-integrated $\chi''$ changes from being independent of $\omega$ in the ordered state to decreasing linearly towards zero as $\omega \rightarrow 0$, as it must in the disordered state. These changes are similar to those observed for spin waves in undoped $La_2CuO_4$ as one warms through the Néel temperature.[45] In the latter case, the dynamical spin correlations in the paramagnetic state are viewed as evidence of instantaneous spin correlations with the character of the Néel state but without the static order.[46,47] By analogy, we take the low-energy IC spin fluctuations in the LTO phase of LBCO to be evidence of instantaneous stripe correlations of the same type that become ordered in the LTT phase.[19] Given that the nuclear displacements induced by charge order represent a primary order parameter for the stripe-ordered state,[6,48] we conclude that IC spin fluctuations in the LTO phase are evidence of dynamic charge stripes.[19] The relevance to other cuprates will be discussed.

A surprising feature observed in the ordered state is a dispersion of the inelastic IC scattering towards the AF wave vector with increasing $\omega$. This is different from the behavior that is observed for spin waves in stripe-ordered $La_{2-x}Sr_xNiO_{4+\delta}$.[49–52] This mystery has been resolved in a separate study,[53] where we measured the spin excitations up to ~200 meV and found that their dispersion is incompatible with semiclassical spin-wave theory.[40–44] Instead, it appears that the full spectrum can be understood in terms of a model of weakly coupled two-leg AF spin ladders.[54–56]

Besides dispersing with energy, the apparent incommensurability $\delta$ is temperature dependent. There is a sharp drop in $\delta$ at the LTT-LTO transition and then a more gradual decrease with increasing temperature. (A similar result has been observed recently in LNSCO.[57]) Complementary reciprocal-space maps of the magnetic scattering at $\hbar\omega$ =4 meV have been obtained at several temperatures for a sample of $La_{1.875}Ba_{0.075}Sr_{0.050}CuO_4$. We show that the latter results can be reproduced by a disordered stripe model, with a temperature-dependent average stripe period. These results may be of interest for interpreting the charge ordering effects observed in $Bi_2Sr_2CaCu_2O_{8+\delta}$ by scanning tunneling spectroscopy (STS).[19,58–60]

The format of this paper is as follows. Sample preparation and experimental details are described in Sec. II. The results of neutron scattering measurements and the simulations based on the disordered stripe model which reproduce the temperature dependences of observed inelastic signal will be presented in Secs. III and IV, respectively. Then, we discuss the results and their relevance to understanding other cuprate superconductors in Sec. V. Finally, our results are briefly summarized in Sec. VI.

## II. SAMPLE PREPARATION AND EXPERIMENTAL DETAILS

Sizable single crystals of $La_{1.875}Ba_{0.125}CuO_4$ and $La_{1.875}Ba_{0.075}Sr_{0.050}CuO_4$ were grown by a traveling-solvent floating-zone method. The feed rod was prepared by the conventional solid-state method. Dried powders of $La_2O_3$, $BaCO_3$, $SrCO_3$, and CuO (99.99% purity) were mixed with the nominal molar ratio of La:(Ba,Sr):Cu=1.875:0.125:1 and calcined at 860, 920, and 960 °C for 24 h in air with intermediate grindings. After this procedure, we added extra $BaCO_3$ and CuO of 0.5 and 1.5 mol. %, respectively, into calcined powder in order to compensate the loss of these components during the following crystal growth. Mixed powder was formed into cylindrical rods 8 mm in diameter and 150 mm in length. The rods were hydrostatically pressed and then sintered at 1250 °C for 24 h in air. We used a solvent with a composition of La:Ba:Cu=1:1:4 (typically 350 mg in weight) and a $La_{1.88}Sr_{0.12}CuO_4$ single crystal (~8 mm in diameter and 20 mm in length) as a seed rod.

The crystal growth was performed using an infrared radiation furnace (NEC Machinery Co., SC-N35HD) equipped with two large focusing mirrors and small halogen lamps. This combination of mirrors and lamps yields a sharp temperature gradient around the molten zone, which helps to provide stable conditions during the growth.[61] Both the feed and seed rods were rotating (20/25 rpm and counter to one another) to ensure efficient mixing of the liquid and a homogeneous temperature distribution in the molten zone. We set the growth rate at 0.7 mm/h and flowed oxygen gas with a flow rate of 100 $cm^3$/min. These growth conditions are essentially the same as those used for the growth of LSCO crystals.[62] In due time, we successfully obtained a 100-mm-long crystal rod. The initial part of the grown rods (~60 mm for LBCO and ~30 mm for LBSCO), however, broke into powder, possibly due to the inclusion of an impurity phase such as $La_2O_3$ and/or $(La,Ba)_2Cu_2O_5$. The samples for magnetic susceptibility and neutron scattering measurements were cut from the final part of the grown rod. Crystals were subsequently annealed to minimize oxygen deficiencies in the same manner used for LSCO.[62]

Figure 1 shows the magnetic susceptibilities measured using a SQUID (superconducting quantum interference device) magnetometer. In the LBCO sample, the field-shielding effect at low temperature is smaller, and the $T_c$ of 4 K is lower, compared with those reported for $La_{1.89}Ba_{0.11}CuO_4$.[37] (Here, $T_c$ is defined as the temperature where the extrapolated slope of the low-temperature susceptibility intersects zero.) These results demonstrate the suppression of superconductivity in the present LBCO crystal. For further sample characterization, we determined the structural transition temperatures by neutron diffraction. With decreasing temperature, the crystal structure successively changes from a high-temperature-tetragonal (HTT, $I4/mmm$ symmetry) to a low-temperature-orthorhombic (LTO, *Bmab* symmetry) phase at ~250 K, and LTO to low-temperature-tetragonal (LTT, $P4_2/ncm$ symmetry) phase at 60 K [Fig. 4(a)], consistent with results obtained previously on powder samples.[34,63] The former transition temperature is especially sensitive to the Ba concentration; therefore, these results indicate that the Ba

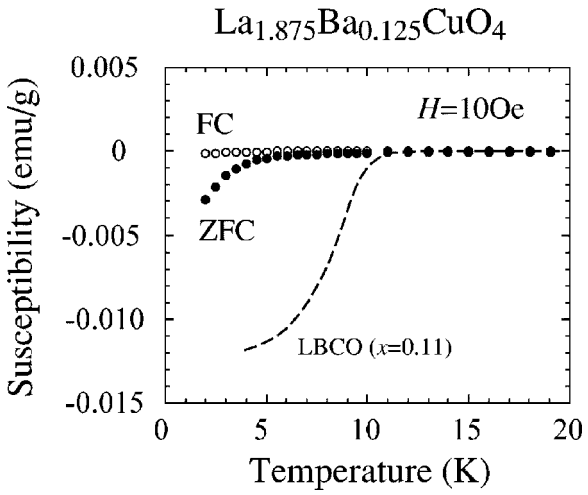


FIG. 1. Zero-field-cooled (ZFC) and field-cooled (FC) susceptibility of $La_{1.875}Ba_{0.125}CuO_4$ single crystal measured at 10 Oe. ZFC susceptibility of $La_{1.89}Ba_{0.11}CuO_4$, taken from Ref. 37, is shown as a reference.

concentration in the present sample is approximately the same as the nominal concentration. More precise Ba content determined by chemical analysis will be presented in a separate paper.[38] The newly grown $La_{1.875}Ba_{0.075}Sr_{0.050}CuO_4$ sample ($T_c$=9 K) shows the LTT-LTO phase transitions at 37 K, with spin and charge order disappearing with the structural transition upon warming. These results are identical to those for the sample used in our earlier elastic neutron scattering study.[35]

Neutron scattering measurements were performed on the Tohoku University triple-axis spectrometer, TOPAN, installed at the JRR-3 reactor in the Japan Atomic Energy Research Institute (JAERI). We selected final neutron energies $E_f$ of 14.7 meV with the collimator sequences of 15′(30′) -30′-30′-180′, and 13.5 meV with 50′-100′-60′-180′, for elastic and inelastic measurements, respectively. Additionally, pyrolytic graphite and sapphire filters were placed in the beam in order to eliminate higher-order neutrons. The columnar-shaped LBCO crystal (~8 mm in diameter and 20 mm in length) was mounted with the (*hk*0) zone parallel to the scattering plane. The measurements were performed below 200 K using a $^4$He-closed-cycle refrigerator. The crystal of $La_{1.875}Ba_{0.075}Sr_{0.050}CuO_4$ (~8 mm in diameter and 15 mm in length) was studied on the thermal-guide triple-axis spectrometer IN22, equipped with a double-focusing analyzer, at the Institut Laue Langevin. For those measurements, we used no collimators and a PG filter was placed after the sample, with $E_f$=14.7 meV.

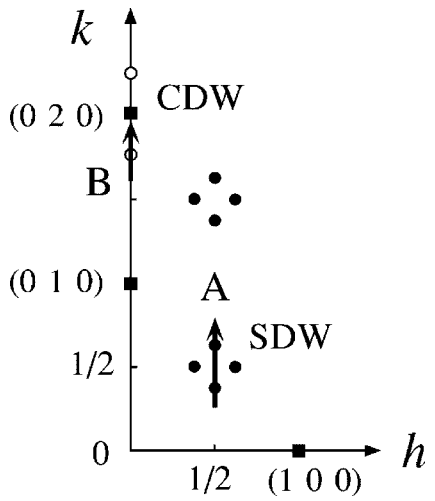


FIG. 2. Scan geometry in the (*hk*0) tetragonal plane. Solid squares show nuclear Bragg peaks; open and solid circles denote nuclear and magnetic IC superlattice peaks, respectively.

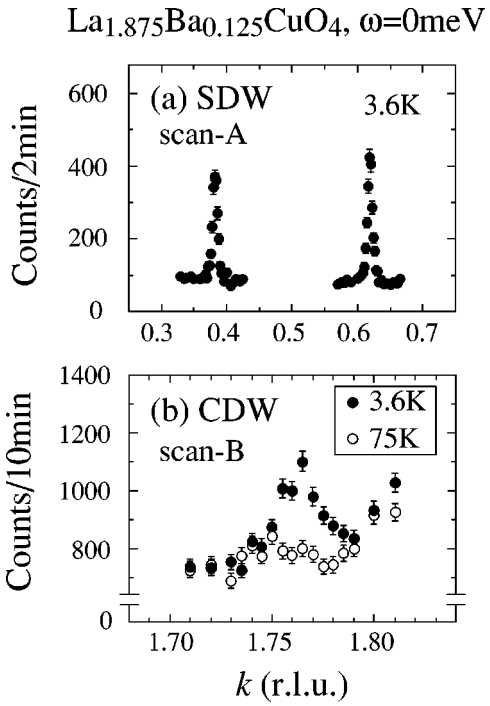


FIG. 3. IC peaks from (a) SDW order (measured along the path labeled A in Fig. 2) and (b) CDW order (measured along path B) in $La_{1.875}Ba_{0.125}CuO_4$. Solid (open) circles indicate measurements below (above) $T_{st}$.

In this paper, since the crystal structure of both samples at low temperature is LTT, with an in-plane lattice constant of 3.78 Å (4 K), we denote the crystallographic indices by using tetragonal notation (1 rlu=1.66 Å$^{-1}$). Most of the inelastic scans for $La_{1.875}Ba_{0.125}CuO_4$ were done along $\mathbf{Q}=(0.5,k,0)$ (denoted as scan A in Fig. 2), which corresponds to a direction perpendicular to the spin and charge stripes. Therefore, the profiles are expected to provide information on the stripe periodicity and correlation length.

## III. RESULTS FOR LBCO

### A. Static correlations

Before investigating the spin fluctuations, we first characterize the static stripe order in the LBCO sample with $x=1/8$. As shown in Fig. 3, both spin-density-wave (SDW) and charge-density-wave (CDW) superlattice peaks were observed at low temperature, consistent with the observations for LNSCO and LBSCO.[6,27,28,35,48,64–67] Both the SDW and

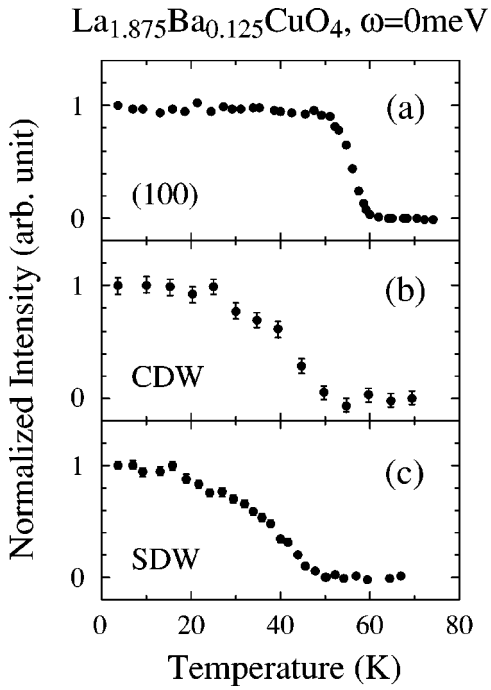


FIG. 4. Temperature dependences of (a) (100), (b) CDW, and (c) SDW superlattice peak intensities in $La_{1.875}Ba_{0.125}CuO_4$.

CDW peak widths are resolution limited, corresponding to correlation lengths $\xi_m \geqslant 150$ Å for the magnetic correlations and $\xi_{ch} \geqslant 60$ Å for the lattice modulations. We note that the SDW and CDW peaks are found to be located at highly-symmetric positions of $(0.5\pm\delta,0.5,0)/(0.5,0.5\pm\delta,0)$ and $(2\pm\varepsilon,0,0)$, respectively, where $\delta=0.118$ and $\varepsilon=0.236=2\delta$. Therefore, the SDW and CDW wave vectors are parallel or perpendicular to the Cu-O bond directions, as found for the tetragonal phases of $La_{1.48}Nd_{0.4}Sr_{0.12}CuO_4$[6,27,28] and $La_{1.875}Ba_{0.075}Sr_{0.050}CuO_4$.[64]

Upon heating, the intensity of the (100) superlattice peak associated with the LTT structure decreases rapidly above 50 K and disappears at $T_{d2}=60$ K because of the structural change into the LTO phase [Fig. 4(a)]. On the other hand, both the CDW and SDW order parameters exhibit second-order-like behavior, and the peak intensities simultaneously vanish at $T_{st}=50$ K [Figs. 4(b) and 4(c)]. The coincident behavior of the two order parameters is similar to the case of LBSCO but different from the result for LNSCO, where the SDW order first disappears followed by the disappearance of CDW order just below $T_{d2}$ upon heating.[6,28,48] In contrast with the onset of the SDW and CDW orders triggered immediately by the LTT structure in LBSCO,[35,68] however, $T_{st}$ is obviously lower than $T_{d2}$ in the present sample. The apparently simultaneous onset of magnetic and charge order in $La_{1.875}Ba_{0.125}CuO_4$ indicates the strong correlation between these two types of order; however, we note that muon-spin-rotation measurements[69] on a polycrystalline sample suggest that true static magnetic order occurs only below 32 K.

### B. Dynamical correlations

Next, we focus our attention on the spin fluctuations. Figure 5 shows the constant-energy spectra for $\hbar\omega=3$ meV

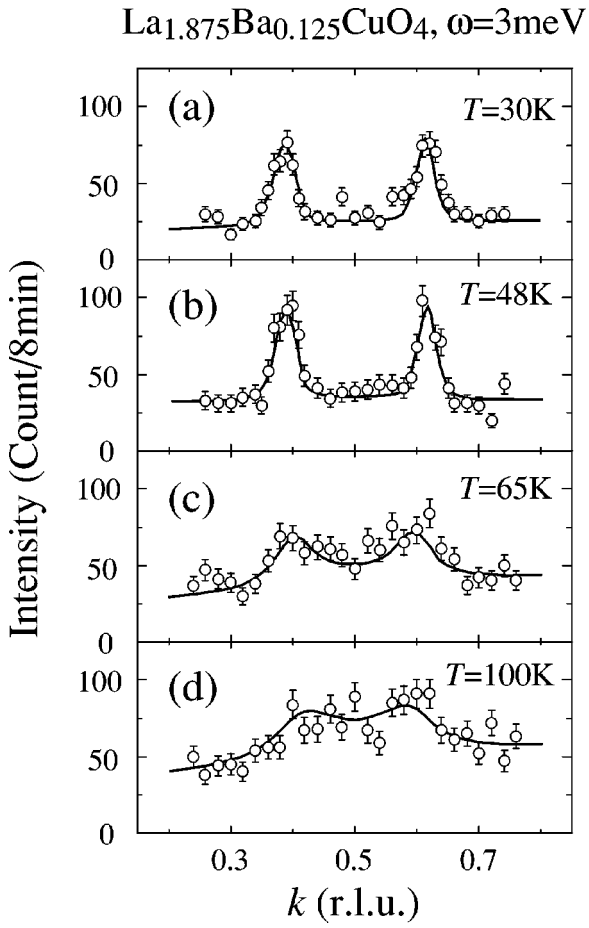


FIG. 5. Inelastic neutron scattering spectra of $La_{1.875}Ba_{0.125}CuO_4$ at (a) 30 K, (b) 48 K, (c) 65 K and (d) 100 K at a constant energy of 3 meV. The solid lines are fits assuming four equivalent peaks at $(0.5\pm\delta,0.5,0)$ and $(0.5,0.5\pm\delta,0)$.

measured at various temperatures. In the stripe-ordered phase at 30 K, the inelastic signal is peaked at the same wave vectors as in the elastic scan, and the width is the resolution-limited width. With increasing temperature, the distance between the pair of IC peaks narrows and the peak width grows.

Figure 6 shows a similar series of scans measured at an excitation energy of 6 meV. Again, sharp IC peaks are observed at $(0.5,0.5\pm0.118,0)$ in the stripe-ordered phase, while the peaks broaden and appear to merge with increasing temperature. Note that the IC peaks measured with $\hbar\omega=6$ meV remain reasonably well-defined at 100 K, while the 3 meV scan yields something closer to a single broad peak at this temperature. We note that the $Q$ resolution at $\omega=3$ meV and 6 meV is comparable. Thus, the lower-energy IC spin fluctuations more easily lose their coherence in the disordered state.

For quantitative analysis, we assume that the magnetic excitations consist of four rods running along the $c^*$ axis and parametrize $\chi''(\mathbf{Q},\omega)$, which is proportional to the magnetic cross section via $S(\mathbf{Q},\omega)=(1-e^{-\hbar\omega/k_BT})^{-1}\chi''(\mathbf{Q},\omega)$, as follows:

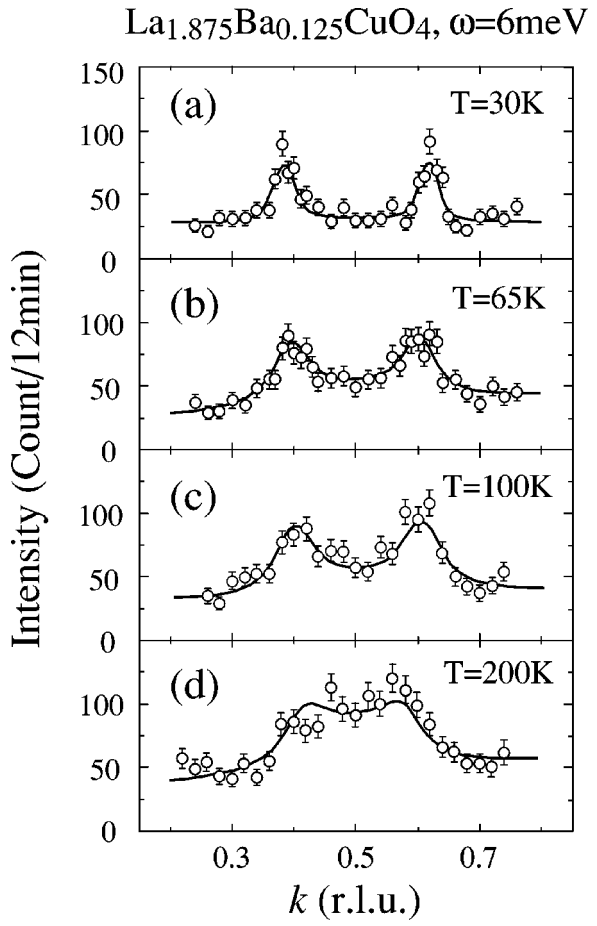


FIG. 6. Inelastic neutron scattering spectra of $La_{1.875}Ba_{0.125}CuO_4$ at (a) 30 K, (b) 65 K, (c) 100 K and (d) 200 K at a constant energy of 6 meV. The solid lines are fits assuming four equivalent peaks at $(0.5\pm\delta,0.5,0)$ and $(0.5,0.5\pm\delta,0)$.

$$\chi''(\mathbf{Q},\omega)=\chi''(\omega)\sum_{n=1}^{4}\frac{\kappa}{(\mathbf{Q}-\mathbf{Q}_{\delta,n})^2+\kappa^2}, \tag{1}$$

where $\mathbf{Q}_{\delta,n}$ represents the four IC wave vectors $[(0.5\pm\delta,0.5,0)/(0.5,0.5\pm\delta,0)]$, $\kappa$ is the peak half width at half maximum, and $\chi''$ is proportional to the integral of $\chi''(\mathbf{Q},\omega)$ over $\mathbf{Q}$ in the $(hk0)$ scattering plane. Measured spectra are fitted to the above function while taking into account the experimental resolution and a background linear in $k$.

Figure 7 shows the frequency dependence of $\chi''(\omega)$ for a number of temperatures. In the stripe-ordered state ($T=8$ K and 30 K), it is independent of $\omega$, just as one would expect for spin waves. In going from 30 K (below $T_{st}$) to 65 K (just above $T_{d2}$), there is little change in $\chi''$ for $\hbar\omega\gtrsim 8$ meV, but there is a linear decrease towards zero at lower frequencies. At higher temperatures, there is a gradual reduction in the overall scale of $\chi''$. The modest changes observed between 30 K and 65 K indicate that there is no significant change in the nature of the fluctuations between the ordered and disordered states. The linear variation of $\chi''$ with $\omega$ for low frequency at 65 K is what one expects to see for spin fluctuations in a disordered spin system. It is also quite similar to what is observed in the normal state of $La_{1.85}Sr_{0.15}CuO_4$.[70]

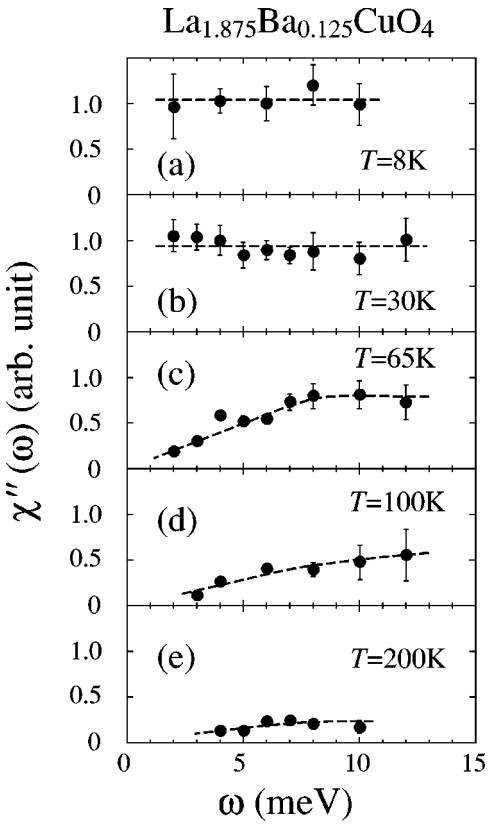


FIG. 7. Local spin susceptibility as a function of $\omega$ in $La_{1.875}Ba_{0.125}CuO_4$ at (a) 8 K, (b) 30 K, (c) 65 K, (d) 100 K, and (e) 200 K. Dashed lines are guides to the eye.

Figure 8 summarizes the results for $\chi''$, $\kappa$, and the incommensurability $\delta$ as a function of temperature for $\hbar\omega=3$ and 6 meV. The temperature dependences of all parameters exhibit a sharp kink at $T_{d2}$, rather than at $T_{st}$, although $\chi''$ starts to decrease at $T_{st}$ upon warming due to the disappearance of magnetic order. The changes are clearly larger at the smaller energy, where one is more sensitive to the proximity to static order. The jump in incommensurability at $T_{d2}$ suggests a lock-in effect, with the stripe spacing adjusting to be commensurate with the modulated lattice potential that pins the stripes in the LTT phase.[71] The general decrease in $\delta$ with increasing temperature was also seen in a recent study of $\frac{1}{8}$-doped LNSCO.[57]

Figure 9 shows the frequency dependence of $\delta$ and $\kappa$ evaluated at 30 K, 65 K, and 200 K. At 30 K, in the stripe-ordered phase, $\delta$ gradually decreases with increasing $\omega$. Even in the low-energy region, $\delta$ is slightly smaller than the value of 0.125 expected from the linear relation between the hole density and $\delta$,[5,27] possibly due to the meandering of stripes and/or disorder in the stripe spacing.[72,73] Above $T_{d2}$ there is a systematic shift in $\delta$ for all $\omega$. The dispersion of $\delta$ appears to have disappeared by the time one reaches 200 K.

The peak half width $\kappa$ shows different behavior. At 30 K, in the stripe-ordered state, $\kappa$ increases roughly linearly in frequency. This behavior might result from unresolved dispersion of counter propagating spin-wave modes. On warm-

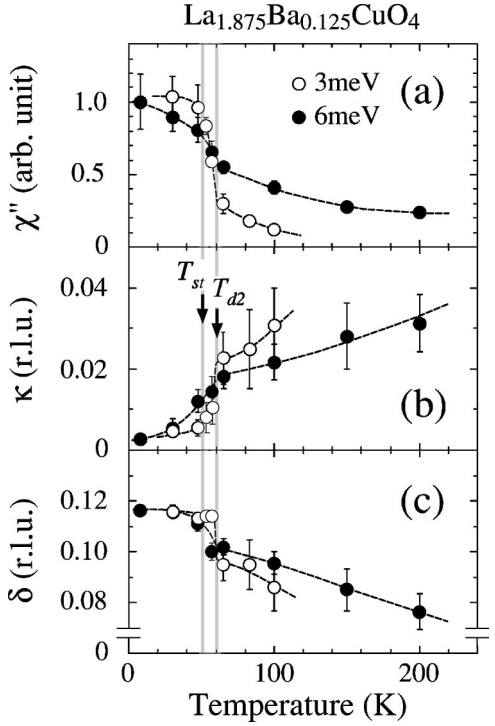


FIG. 8. Temperature dependences of (a) local spin susceptibility $\chi''$, (b) peak width (half width at half maximum) $\kappa$, and (c) incommensurability $\delta$ at the energy transfers of 3 and 6 meV in $La_{1.875}Ba_{0.125}CuO_4$. Vertical lines indicate $T_{st}$ and $T_{d2}$. Dashed lines are guides to the eye.

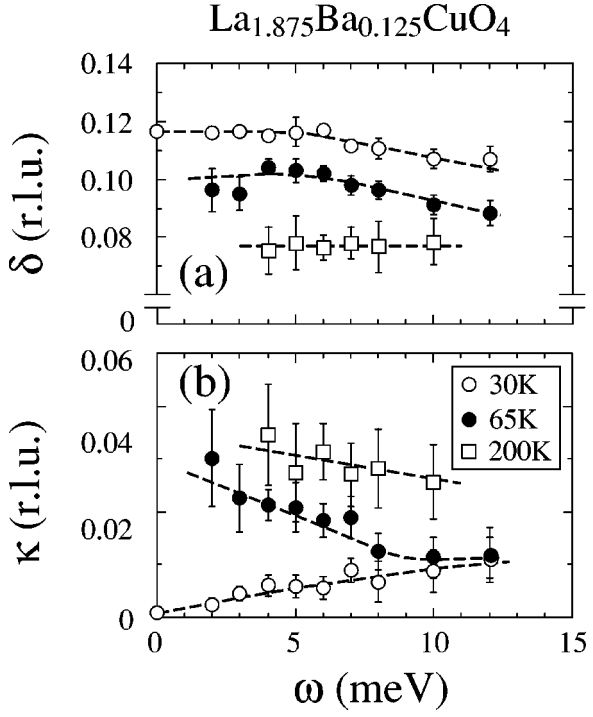


FIG. 9. $\omega$ dependence of (a) incommensurability $\delta$ and (b) resolution-corrected peak width (half width at half maximum) $\kappa$ of IC peaks for $La_{1.875}Ba_{0.125}CuO_4$. Open circles denote 30-K data; solid circles, 65 K; open squares, 200 K.

ing into the disordered state at 65 K, $\kappa$ grows by a large amount at low frequencies, but changes relatively little for $\hbar\omega \gtrsim 8$ meV. Now, this measurement is just along a direction perpendicular to the stripes. To check for anisotropy, we also measured the **Q**-width of the inelastic scattering for $\hbar\omega = 4$ meV at 30 K and 65 K for a direction parallel to the stripes. At 30 K the peak widths are isotropic within experimental uncertainty; however, at 65 K the width perpendicular to the stripes is roughly twice as large as that parallel to the stripes. Such an anisotropy might result from fluctuations in the stripe spacing. Time restrictions prevented a more comprehensive investigation of the peak-width anisotropy.

## IV. DISORDERED STRIPES IN LBSCO

### A. Experimental measurements

In studying the $La_{1.875}Ba_{0.075}Sr_{0.050}CuO_4$ crystal, we performed mesh scans at an excitation energy of 4 meV, mapping out the magnetic scattering in the neighborhood of $\mathbf{Q}_{AF}=(0.5,0.5,0)$ for several temperatures. All of the measurements were in the LTO phase, where there is no static stripe order. To present the results, it is convenient to change to the orthorhombic coordinate system (the system in which the mesh scans were performed), which is rotated by 45° from the tetragonal one, with a change in the lattice parameter to $a_0=\sqrt{2}a_t$. In this rotated system, $\mathbf{Q}_{AF}$ becomes (1,0,0). The data are shown in Figs. 10(a), 10(c), and 10(e); a temperature-independent background, monotonically varying in **Q**, has been subtracted, and the intensities have been corrected for the **Q** dependence of the $Cu^{2+}$ magnetic form factor.[74] In order to improve the counting statistics, we have assumed four-fold symmetry of the data about $\mathbf{Q}_{AF}$ and have averaged the data over the corresponding rotations and reflections to give Figs. 10(b), 10(d), and 10(e). (The spectrometer resolution used was somewhat coarse, which reduced the data collection time but masked any anisotropy in the peak widths at 40 K.) As one can see, the four peaks shift in towards $\mathbf{Q}_{AF}$ on warming, eventually merging by 200 K.

### B. Model calculations

Given the shifts in the IC magnetic peaks with temperature, we want to test how well the measurements can be described within a stripe model and what the data tell us about the nature of the stripe correlations. We will assume that the **Q** dependence of the low-energy fluctuations reflects the correlations within an instantaneous configuration of disordered stripes. One source of disorder comes from the positions of the charge stripes that define the magnetic domains.[73] Given a particular instantaneous configuration of stripes, we also expect there to be a finite spin-spin correlation length. To combine these two types of disorder, we performed numerical calculations. (We have also considered transverse fluctuations in the stripe positions, but found that the level of agreement with the measurements was not sensitive to this additional form of disorder, so we neglect it here.)

The numerical calculations were performed on an array of $128\times128$ sites. The site **n** was assumed to have either an up

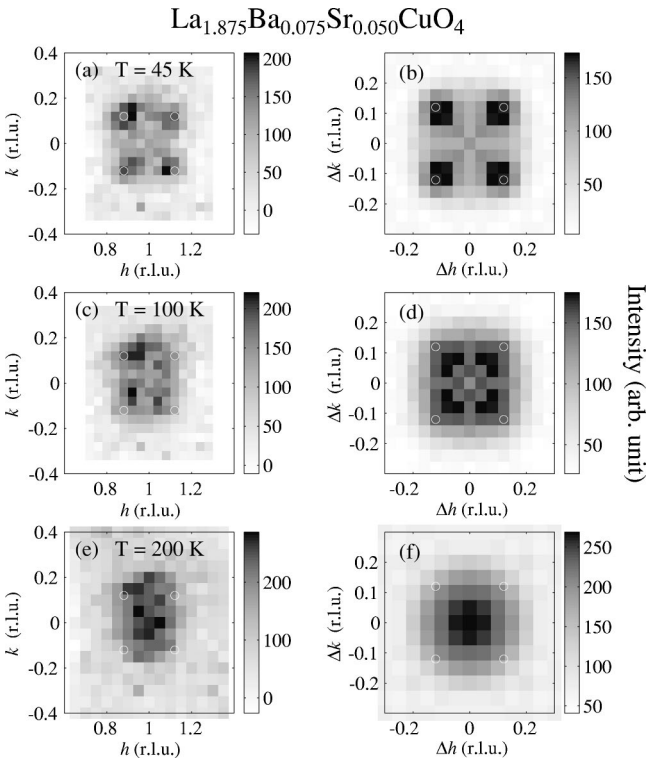


FIG. 10. Mesh scans about $\mathbf{Q}_{AF}$ for $\hbar\omega=4$ meV. (a), (c), and (e) are raw data, after subtraction of background (see text) and correction for the Cu magnetic form factor, at $T=45$, 100, and 200 K, respectively; panels on the right [(b),(d),(f)] were obtained from those on the left by averaging over four-fold symmetry operations. The white circles indicate the positions of the elastic magnetic peaks that appear below 37 K.

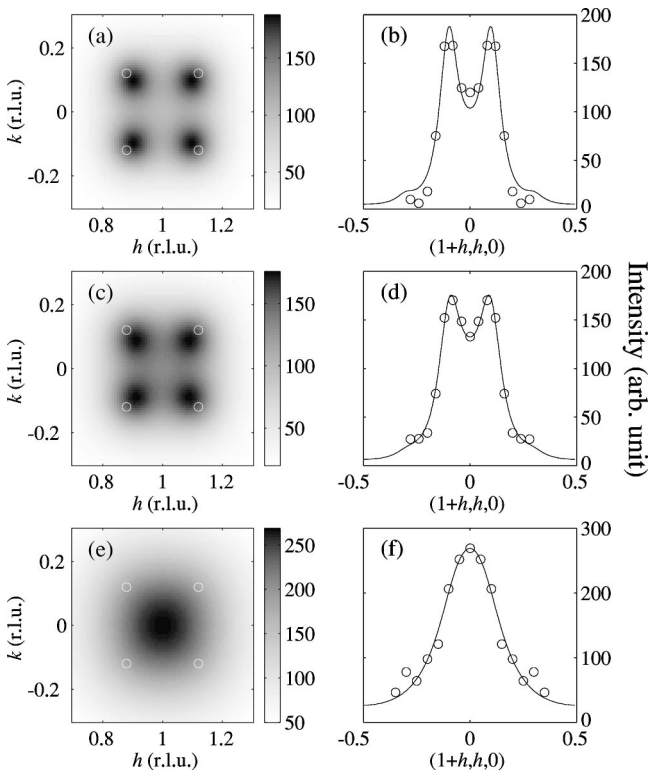


FIG. 11. Simulations of the 4 meV scans, as described in the text. (a), (c), and (e) are simulations of the mesh scans at $T=45$, 100, and 200 K, respectively. (b), (d), and (f) compare the calculated curves with the symmetrized data along $\mathbf{Q}=(1+h,h,0)$. The white circles are the same as in Fig. 10.

or down spin, denoted by $F_{\mathbf{n}}=+1$ or $-1$, or a hole, denoted by 0. Stripes of holes were taken to be straight lines of unit width running in the $y$ direction. The spacings between the stripes were randomly selected to be $j$ or $j+1$ (where $j$ is an integer) with frequencies of the two choices set to give an average spacing $d$ such that $j \leqslant d \leqslant j+1$. For a given configuration, the scattered intensity $I(\mathbf{Q})$ was calculated as

$$I(\mathbf{Q}) = \sum_{\mathbf{m}} \left( \sum_{\mathbf{n}} F_{\mathbf{n}} F^{*}_{\mathbf{n}+\mathbf{m}} \right) e^{i\mathbf{Q}\cdot\mathbf{m}} e^{-\kappa_s |\mathbf{m}|}, \qquad (2)$$

where the exponential decay factor is intended to describe the spatial falloff of spin-spin correlations. The calculated intensity contains just a pair of peaks, since the model has a unique stripe orientation. To compare with the measurements, we have rotated the intensity pattern by 90° and added it to the original version.

In simulating the measurements, we have not made any correction for the spectrometer resolution, which dominates the $Q$ width of the signal at 45 K. The finite resolution, which is convolved with the sample scattering in reciprocal space, effectively acts like another correlation decay factor in real space; in ignoring the resolution, we compensate by overestimating the inverse correlation length $\kappa_s$. The simulations are shown in Fig. 11. At each temperature, the parameters $d$ and $\kappa_s$ were determined by a least-squares fit to the data along the line $\mathbf{Q}=(1+h,h,0)$; the comparison of the data and simulations along this line is shown in Figs. 11(b), 11(d), and 11(f). The parameter values for each temperature are listed in Table I. The disordered stripe model appears to give an adequate description of the data.

One key result of the modeling is that one must allow for a significant change in the stripe spacing from that in the ordered state in order to get a reasonable fit to the data. A second important conclusion regarding the stripe model is that the scattering becomes commensurate as the correlation length [$=1/(2\pi\kappa_s)$ in lattice units] becomes smaller than half of the stripe spacing. In this case, the magnetic scattering comes largely from a single magnetic domain, and there is no longer any significant cancellation at the commensurate wave vector due to scattering from neighboring antiphase domains. Obviously, when the scattering becomes commen-

TABLE I. Parameter values determined by fitting simulations to data. $d$ is expressed in lattice units and $\kappa$ in rlu, both for the tetragonal cell.

| $T$ (K) | $d$ | $\kappa_s$ (rlu) |
|---|---|---|
| 45 | 5.0±0.4 | 0.06±0.01 |
| 100 | 5.2±0.4 | 0.07±0.01 |
| 200 | 7.1±1.4 | 0.14±0.03 |

surate, there is no longer any unique signature of stripe correlations; nevertheless, instantaneous charge stripe correlations are compatible with commensurate magnetic fluctuations.

The values of the average stripe spacing required to describe the measurements in the disordered state are significantly longer than the value of $\approx 4$ that is characteristic of the ordered state. How can we understand this? Transverse fluctuations of a given stripe increase its arc length.[83] If the hole density per arc length remains roughly the same as in the ordered state, then there must be more holes within each stripe. That, in turn, implies a lower density of stripes within a $CuO_2$ plane and, hence, an increased stripe spacing. Repulsive Coulomb interactions between stripes would also tend to favor increased average stripe spacings when transverse fluctuations are important. The fact that adequate simulations of the scattering measurements do not require explicit inclusion of the transverse meanderings may simply indicate that the spin-spin correlation length is shorter than the typical distance between transverse stripe displacements.

## V. DISCUSSION

Our results indicate that the spin correlations in the LTO phase of $La_{1.875}Ba_{0.125}CuO_4$ are a dynamic form of the ordered state found at lower temperatures in the LTT phase. The low-temperature phase is characterized by charge stripe order. While magnetic order appears to have the same onset temperature (50 K), a muon-spin-rotation study has shown that the true static order appears only below 30 K.[69] From the perspective of doped antiferromagnets, stripe order involves a spatial segregation of doped holes that allows a persistence of hole-poor, AF-insulator regions. We have obtained direct evidence for the existence of a dynamic, fluctuating stripe phase in LBCO. A related dynamic stripe phase has been detected previously in $La_{2-x}Sr_xNiO_4$,[50,52] so there is a precedent for such behavior.

The abrupt change in the incommensurability at $T_{d2}$ may allow an improved understanding of the striking behavior of the Hall coefficient measured by Noda, Eisaki, and Uchida[7] in $La_{1.4-x}Nd_{0.6}Sr_xCuO_4$. For that system, the Hall coefficient behaved "normally" (i.e., looked similar to comparably doped LSCO) in the LTO phase, but dropped rapidly towards zero on cooling through the transition to the LTT phase for $x \leqslant 0.13$. The behavior in the LTT phase has been explained in terms of the response of charge stripes with a doped-hole concentration of 0.5 per Cu site. For such a condition, there is electron-hole symmetry within a stripe, and consequently the Hall coefficient should be zero.[75,76] The electron-hole symmetry is quite sensitive to the hole concentration in the stripes, and hence it should be sensitive to the incommensurability, which will affect the hole concentration. The jump in the incommensurability that we observe at the structural transition implies a jump in the hole concentration within the stripes, assuming that all holes remain in stripes. (Even if the average hole concentration within stripes remains roughly the same due to meandering of the stripes in the disordered phase, there may still be enough change to eliminate the particle-hole symmetry.) It is reasonable to expect similar behavior in $La_{1.4-x}Nd_{0.6}Sr_xCuO_4$, so that the abrupt change in the Hall coefficient likely reflects the difference in hole concentration for dynamic stripes versus that in static stripes.

Recent analyses of the Hubbard model using methods beyond Hartree-Fock have yielded stripe solutions that are quite similar to experimental observations.[77–81] A first-principles calculation for $\frac{1}{8}$-doped LSCO using the LDA+U method yields bond-centered charge stripes;[82] the superexchange interactions calculated within the hole-poor ladders are comparable to what we have obtained from measurements of the magnetic excitations in LBCO at higher energies.[53] Thus, there is growing theoretical support for the concept of stripe correlations as a natural consequence of doping holes into an antiferromagnetic insulator. Quantum fluctuations (and the absence of a pinning potential) lead to the stripe-liquid state.[18,83–86]

### A. Relevance to LSCO

The low-energy magnetic fluctuations found in the normal state of LSCO (Ref. 70) look quantitatively similar to what we have measured in the LTO phase of LBCO. Elastic IC magnetic peaks can be induced in underdoped LSCO at low temperature through Zn doping[87] or by applying a magnetic field along the *c* axis.[88,89] The simplest explanation for all of the these observations is that dynamic charge stripes are present in LSCO and that they can be pinned by local defects.[90]

Weaknesses in the Fermi-surface-nesting explanation for the IC spin fluctuations in LSCO have been discussed by Kivelson *et al.*[19] Given the experimental evidence for the dynamic stripe phase presented here, we believe that the Fermi-surface-nesting approach is no longer tenable for interpreting results in LSCO. Rather than trying to explain the IC spin correlations in terms of the shape of the Fermi surface, one must strive to understand photoemission measurements of the electronic spectral function near the Fermi surface[91,92] in terms of the slowly fluctuating charge stripes.

The gapless spin fluctuations in the normal state of LSCO indicate that the charge stripes must fluctuate quite slowly. This raises the question of whether there is some feature of LSCO that might control the fluctuation rate. An old, but still plausible, idea is that the charge stripes may couple to the octahedral tilt mode that is associated with the transformation from the LTO to the LTT phase. This mode has an energy of just a couple of meV.[93] It softens on cooling below 100 K, but the softening ends at $T_c$.[94,95] A hardening of the elastic constant $(C_{11}-C_{12})/2$ below $T_c$ was found to be reduced by the lowering of $T_c$ through application of a magnetic field.[96] Thus, it seems quite possible that charge stripes in LSCO are coupled to slow LTT-like fluctuations of the lattice.

### B. Relevance to YBCO

There has long been a recognition of similarities in the low-energy magnetic scattering of well-underdoped YBCO with that of LSCO,[97,98] and measurements to higher energies made clear similarities to antiferromagnetic dispersions.[99] The clear identification of incommensurate magnetic scatter-

ing at $\sim 24$ meV in $YBa_2Cu_3O_{6.6}$ by Mook and co-workers.[100–102] made the connection to LSCO stronger. Recent studies have provided strong evidence for stripe-like spin excitations in detwinned crystals of $YBa_2Cu_3O_{6.5}$,[103] and for both charge and spin modulations in $YBa_2Cu_3O_{6.35}$.[104]

Objections to the dynamic stripe picture have come from studies of spin excitations in YBCO samples closer to optimal doping.[105] There the excitations observed in the superconducting state are incompatible with semiclassical spin waves from stripes.[40–44] An interpretation of these features based on Fermi-surface-nesting effects has been preferred.[24,105,106] Our study of the high-energy spin excitations in LBCO removes the objection to a stripe interpretation, as the results are quite different from the predictions of semiclassical spin-wave models. In fact, our results for LBCO show striking similarities to recent measurements on YBCO samples with a range of dopings.[107–109] Thus, it appears that the dynamic stripe scenario provides a universal approach for understanding most features of the magnetic excitation spectrum in the two most carefully studied systems, YBCO and LSCO. The magnetic resonance phenomenon is one feature that is not yet explained by this approach.

There is one apparent difference between LSCO and YBCO that can be explained by the dispersion of the low-energy spin excitations. In LSCO, the incommensurability $\delta$, measured at $\sim 3$ meV, varies linearly with doping up to a hole concentration $p \approx \frac{1}{8}$, and it saturates at $\delta \sim \frac{1}{8}$ for larger $p$.[5] In YBCO there is a substantial spin gap that grows with $p$, and hence one must measure $\delta$ at relatively high energies ($>30$ meV near optimum doping). Dai *et al.*[110] found that $\delta$ saturates at $\sim \frac{1}{10}$ for $p > 0.10$, which is different from the LSCO result. Taking the dispersion of the spin excitations into account should reduce this apparent discrepancy.

### C. Relevance to STS studies

Scanning tunneling spectroscopy studies on $Bi_2Sr_2CaCu_2O_{8+\delta}$ have identified spatial modulations of electronic states at low energies (within the superconducting gap).[19,58–60] Some of the spatially modulated features disperse with bias voltage, and these appear to be associated with scattering of electronic excitations across the gapped Fermi surface.[59,60] Certain features, however, involve modulations oriented parallel to the Cu-O bonds with a period of approximately $4a$, suggesting a connection with the type of charge stripe order that we have discussed here.[19,58,59,111] The relevant STS modulations do not always have a period of exactly $4a$. The period varies slightly from sample to sample and may increase a bit with temperature. Here we point out that such behavior is quite consistent with the temperature-dependent incommensurability in LBCO and with the doping dependent incommensurability in LSCO.[5]

## VI. SUMMARY

We have presented a neutron scattering study of stripe order and fluctuations in single crystals of $La_{1.875}Ba_{0.125}CuO_4$ and $La_{1.875}Ba_{0.075}Sr_{0.050}CuO_4$. Charge and spin stripe order are observed only within the LTT phase. The **Q**-integrated dynamic susceptibility is frequency independent in the ordered state, consistent with spin waves; however, the spin excitations disperse inwards towards $\mathbf{Q}_{AF}$ with increasing energy in an anisotropic manner that is not expected in a semiclassical model.

The IC spin excitations evolve continuously through the LTT-LTO transition. For $\hbar\omega \sim 10$ meV, there is essentially no change in the local susceptibility through the transition, indicating that the character of the excitations in the disordered state is the same as in the ordered state, where the spin incommensurability is tied to the presence of charge stripes. Our measurements provide clear evidence for dynamic charge stripes in the LTO phase. We have discussed the relevance of our results for interpreting the magnetic excitations observed in LSCO and YBCO.

## ACKNOWLEDGMENTS

We thank H. Kimura, K. Machida, M. Matsuda, G. Shirane, H. Yamase, I. Watanabe, and G. Xu for valuable discussions. This work was supported in part by the Japanese Ministry of Education, Culture, Sports, Science and Technology, Grant-in-Aid for Scientific Research on Priority Areas (Novel Quantum Phenomena in Transition Metal Oxides), No. 12046239, 2000, for Scientific Research (A), No. 10304026, 2000, for Encouragement of Young Scientists, No. 13740216, 2001, and for Creative Scientific Research No. (13NP0201) "Collaboratory on Electron Correlations—Toward a New Research Network between Physics and Chemistry," by the Japan Science and Technology Corporation, the Core Research for Evolutional Science and Technology Project (CREST). J.M.T. is supported at Brookhaven by the Office of Science, U.S. Department of Energy, through Contract No. DE-AC02-98CH10886.

*Electronic address: fujita@imr.tohoku.ac.jp

[1] M. A. Kastner, R. J. Birgeneau, G. Shirane, and Y. Endoh, Rev. Mod. Phys. **70**, 897 (1998).

[2] H. Yoshizawa, S. Mitsuda, H. Kitazawa, and K. Katsumata, J. Phys. Soc. Jpn. **57**, 3686 (1988).

[3] R. J. Birgeneau, Y. Endoh, Y. Hidaka, K. Kakurai, M. A. Kastner, T. Murakami, G. Shirane, T. R. Thurston, and K. Yamada, Phys. Rev. B **39**, 2868 (1989).

[4] S.-W. Cheong, G. Aeppli, T. E. Mason, H. Mook, S. M. Hayden, P. C. Canfield, Z. Fisk, K. N. Clausen, and J. L. Martinez, Phys. Rev. Lett. **67**, 1791 (1991).

[5] K. Yamada, C. H. Lee, K. Kurahashi, J. Wada, S. Wakimoto, S. Ueki, H. Kimura, Y. Endoh, S. Hosoya, G. Shirane, R. J. Birgeneau, M. Greven, M. A. Kastner, and Y. J. Kim, Phys. Rev. B **57**, 6165 (1998).

[6] J. M. Tranquada, B. J. Sternlieb, J. D. Axe, Y. Nakamura, and S.

Uchida, Nature (London) **375**, 561 (1995).
[7] T. Noda, H. Eisaki, and S. Uchida, Science **286**, 265 (1999).
[8] X. J. Zhou, P. Bogdanov, S. A. Kellar, T. Noda, H. Eisaki, S. Uchida, Z. Hussain, and Z.-X. Shen, Science **286**, 268 (1999).
[9] Y. Ando, A. N Lavrov, S. Komiya, K. Segawa, and X. F. Sun, Phys. Rev. Lett. **87**, 017001 (2001).
[10] V. J. Emery, S. A. Kivelson, and O. Zachar, Phys. Rev. B **56**, 6120 (1997).
[11] C. Castellani, C. Di Castro, and M. Grilli, Z. Phys. B: Condens. Matter **103**, 137 (1997).
[12] M. Vojta and S. Sachdev, Phys. Rev. Lett. **83**, 3916 (1999).
[13] J. Orenstein and A. J. Millis, Science **288**, 468 (2000).
[14] J. Zaanen, O. Y. Osman, H. V. Kruis, Z. Nussinov, and J. Tworzydło, Philos. Mag. B **81**, 1485 (2001).
[15] A. H. Castro Neto, Phys. Rev. B **64**, 104509 (2001).
[16] E. W. Carlson, V. J. Emery, S. A. Kivelson, and D. Orgad, in *The Physics of Superconductors Vol. II: Superconductivity in Nanostructures, High-$T_c$ and Novel Superconductors, Organic Superconductors*, edited by K. H. Bennemann and J. B. Ketterson (Springer-Verlag, Berlin, 2004).
[17] E. Arrigoni, E. Fradkin, and S. A. Kivelson, cond-mat/0309572 (unpublished).
[18] J. Zaanen, M. L. Horbach, and W. van Saarloos, Phys. Rev. B **53**, 8671 (1996).
[19] S. A. Kivelson, I. P. Bindloss, E. Fradkin, V. Oganesyan, J. M. Tranquada, A. Kapitulnik, and C. Howald, Rev. Mod. Phys. **75**, 1201 (2003).
[20] Q. Si, Y. Zha, K. Levin, and J. P. Lu, Phys. Rev. B **47**, 9055 (1993).
[21] P. B. Littlewood, J. Zaanen, G. Aeppli, and H. Monien, Phys. Rev. B **48**, 487 (1993).
[22] F. Mancini, D. Villani, and H. Matsumoto, Phys. Rev. B **57**, 6145 (1998).
[23] K. Kuroki, R. Arita, and H. Aoki, Phys. Rev. B **60**, 9850 (1999).
[24] Y.-J. Kao, Q. Si, and K. Levin, Phys. Rev. B **61**, R11 898 (2000).
[25] Y. Yamase and H. Kohno, J. Phys. Soc. Jpn. **332**, 332 (2000).
[26] F. Yuan, S. Feng, Z.-B. Su, and L. Yu, Phys. Rev. B **64**, 224505 (2001).
[27] J. M. Tranquada, J. D. Axe, N. Ichikawa, A. R. Moodenbaugh, Y. Nakamura, and S. Uchida, Phys. Rev. Lett. **78**, 338 (1997).
[28] N. Ichikawa, S. Uchida, J. M. Tranquada, T. Niemöller, P. M. Gehring, S.-H. Lee, and J. R. Schneider, Phys. Rev. Lett. **85**, 1738 (2000).
[29] J. G. Bednorz and K. A. Müller, Z. Phys. B: Condens. Matter **64**, 189 (1986).
[30] A. R. Moodenbaugh, Y. Xu, M. Suenaga, T. J. Folkerts, and R. N. Shelton, Phys. Rev. B **38**, 4596 (1988).
[31] K. Kumagai, Y. Nakamura, I. Watanabe, Y. Nakamichi, and H. Nakajima, J. Magn. Magn. Mater. **76–77**, 601 (1988).
[32] H. Takagi, T. Ido, S. Ishibashi, M. Uota, S. Uchida, and Y. Tokura, Phys. Rev. B **40**, 2254 (1989).
[33] K. Kumagai, K. Kawano, I. Watanabe, K. Nishiyama, and K. Nagamine, Hyperfine Interact. **86**, 473 (1994).
[34] J. D. Axe, A. H. Moudden, D. Hohlwein, D. E. Cox, K. M. Mohanty, A. R. Moodenbaugh, and Y. Xu, Phys. Rev. Lett. **62**, 2751 (1989).
[35] M. Fujita, H. Goka, K. Yamada, and M. Matsuda, Phys. Rev. Lett. **88**, 167008 (2002).
[36] H. Tanabe, S. Watauchi, I. Tanaka, and H. Kojima, in *Advances in Superconductivity X*, edited by K. Osamura and I. Hirabayashi (Springer, Tokyo, 1998), p. 371.
[37] T. Adachi, T. Noji, and Y. Koike, Phys. Rev. B **64**, 144524 (2001).
[38] H. Goka, M. Fujita, K. Yamada, M. Matsuda, I. Watanabe, and K. Nagamine (unpublished).
[39] N. Hasselmann, A. H. Castro Neto, C. Morais Smith, and Y. Dimashko, Phys. Rev. Lett. **82**, 2135 (1999).
[40] E. Kaneshita, M. Ichioka, and K. Machida, J. Phys. Soc. Jpn. **70**, 866 (2001).
[41] C. D. Batista, G. Ortiz, and A. V. Balatsky, Phys. Rev. B **64**, 172508 (2001).
[42] S. Varlamov and G. Seibold, Phys. Rev. B **65**, 075109 (2002).
[43] F. Krüger and S. Scheidl, Phys. Rev. B **67**, 134512 (2003).
[44] E. W. Carlson, D. X. Yao, and D. K. Campbell, cond-mat/0402231 (unpublished).
[45] K. Yamada, K. Kakurai, Y. Endoh, T. R. Thurston, M. A. Kastner, R. J. Birgeneau, G. Shirane, Y. Hidaka, and T. Murakami, Phys. Rev. B **40**, 4557 (1989).
[46] G. Shirane, Y. Endoh, R. J. Birgeneau, M. A. Kastner, Y. Hidaka, M. Oda, M. Suzuki, and T. Murakami, Phys. Rev. Lett. **59**, 1613 (1987).
[47] S. Chakravarty, B. I. Halperin, and D. R. Nelson, Phys. Rev. Lett. **60**, 1057 (1988).
[48] J. M. Tranquada, J. D. Axe, N. Ichikawa, Y. Nakamura, S. Uchida, and B. Nachumi, Phys. Rev. B **54**, 7489 (1996).
[49] J. M. Tranquada, P. Wochner, and D. J. Buttrey, Phys. Rev. Lett. **79**, 2133 (1997).
[50] P. Bourges, Y. Sidis, M. Braden, K. Nakajima, and J. M. Tranquada, Phys. Rev. Lett. **90**, 147202 (2003).
[51] A. T. Boothroyd, D. Prabhakaran, P. G. Freeman, S. J. S. Lister, M. Enderle, A. Hiess, and J. Kulda, Phys. Rev. B **67**, 100407 (2003).
[52] S.-H. Lee, J. M. Tranquada, K. Yamada, D. J. Buttrey, Q. Li, and S.-W. Cheong, Phys. Rev. Lett. **88**, 126401 (2002).
[53] J. M. Tranquada, H. Woo, T. G. Perring, H. Goka, G. D. Gu, G. Xu, M. Fujita, and K. Yamada, Nature (London) **429**, 534 (2004).
[54] M. Vojta and T. Ulbricht, cond-mat/0402377 (unpublished).
[55] G. S. Uhrig, K. P. Schmidt, and M. Grüninger, cond-mat/0402659 (unpublished).
[56] S. Dalosto and J. Riera, Phys. Rev. B **62**, 928 (2000).
[57] M. Ito, Y. Yasui, S. Iikubo, M. Sato, A. Kobayashi, and K. Kakurai, J. Phys. Soc. Jpn. **72**, 1627 (2003).
[58] C. Howald, H. Eisaki, N. Kaneko, M. Greven, and A. Kapitulnik, Phys. Rev. B **67**, 014533 (2003).
[59] M. Vershinin, S. Misra, S. Ono, Y. Abe, Y. Ando, and A. Yazdani, www.sciencexpress.org, 10.1126/science.1093384.
[60] J. E. Hoffman, E. W. Hudson, K. M. Lang, V. Madhavan, H. Eisaki, S. Uchida, and J. C. Davis, Science **295**, 466 (2002).
[61] C. H. Lee, N. Kaneko, S. Hosoya, K. Kurahashi, S. Wakimoto, K. Yamada, and Y. Endoh, Supercond. Sci. Technol. **11**, 891 (1998).
[62] M. Fujita, K. Yamada, H. Hiraka, P. M. Gehring, S. H. Lee, S. Wakimoto, and G. Shirane, Phys. Rev. B **65**, 064505 (2002).
[63] S. J. L. Billinge, G. H. Kwei, A. C. Lawson, J. D. Thompson, and H. Takagi, Phys. Rev. Lett. **71**, 1903 (1993).
[64] M. Fujita, H. Goka, K. Yamada, and M. Matsuda, Phys. Rev. B **66**, 184503 (2002).
[65] T. Niemöller, N. Ichikawa, T. Frello, H. Hünnefeld, N. H. Andersen, S. Uchida, J. R. Schneider, and J. M. Tranquada, Eur. Phys.

J. B **12**, 509 (1999).
[66] M. v. Zimmermann, A. Vigliante, T. Niemöller, N. Ichikawa, T. Frello, S. Uchida, N. H. Andersen, H. Madsen, P. Wochner, J. M. Tranquada, D. Gibbs, and J. R. Schneider, Europhys. Lett. **41**, 629 (1998).
[67] H. Kimura, H. Goka, M. Fujita, Y. Noda, and K. Yamada, N. Ikeda, Phys. Rev. B **67**, 140503 (2003).
[68] M. Fujita, H. Goka, K. Yamada, and M. Matsuda, Appl. Phys. A: Mater. Sci. Process. **74**, S1638 (2002).
[69] G. M. Luke, L. P. Le, B. J. Sternlieb, W. D. Wu, Y. J. Uemura, J. H. Brewer, T. M. Riseman, S. Ishibashi, and S. Uchida, Physica C **185-189**, 1175 (1991).
[70] C.-H. Lee, K. Yamada, Y. Endoh, G. Shirane, R. J. Birgeneau, M. A. Kastner, M. Greven, and Y.-J. Kim, J. Phys. Soc. Jpn. **69**, 1170 (2000).
[71] N. Hasselmann, A. H. Castro Neto, and C. Morais Smith, Phys. Rev. B **65**, 220511 (2002).
[72] O. Zachar, Phys. Rev. B **62**, 13 836 (2000).
[73] J. M. Tranquada, N. Ichikawa, and S. Uchida, Phys. Rev. B **59**, 14 712 (1999).
[74] S. Shamoto, M. Sato, J. M. Tranquada, B. J. Sternlieb, and G. Shirane, Phys. Rev. B **48**, 13 817 (1993).
[75] V. J. Emery, E. Fradkin, S. A. Kivelson, and T. C. Lubensky, Phys. Rev. Lett. **85**, 2160 (2000).
[76] P. Prelovšek, T. Tohyama, and S. Maekawa, Phys. Rev. B **64**, 052512 (2001).
[77] J. Lorenzana and G. Seibold, Phys. Rev. Lett. **89**, 136401 (2002).
[78] E. Louis, F. Guinea, M. P. López Sancho, and J. A. Vergés, Phys. Rev. B **64**, 205108 (2001).
[79] M. Fleck, A. I. Lichtenstein, E. Pavarini, and A. M. Oleś, Phys. Rev. Lett. **84**, 4962 (2000).
[80] S. R. White and D. J. Scalapino, Phys. Rev. Lett. **91**, 136403 (2003).
[81] M. Ichioka and K. Machida, J. Phys. Soc. Jpn. **68**, 4020 (1999).
[82] V. I. Anisimov, M. A. Korotin, A. S. Mylnikova, A. V. Kozhevnikov, and J. Lorenzana, cond-mat/0402162 (unpublished).
[83] S. A. Kivelson, E. Fradkin, and V. J. Emery, Nature (London) **393**, 550 (1998).
[84] S. Sachdev, Phys. World **12**(4), 33 (1999).
[85] T. Momoi, Phys. Rev. B **67**, 014529 (2003).
[86] G. Schmid and M. Troyer, cond-mat/0304657 (unpublished).
[87] H. Kimura, M. Kofu, Y. Matsumoto, and K. Hirota, Phys. Rev. Lett. **91**, 067002 (2003).
[88] S. Katano, M. Sato, K. Yamada, T. Suzuki, and T. Fukase, Phys. Rev. B **62**, R14 677 (2000).
[89] B. Lake, H. M. Rønnow, N. B. Christiansen, G. Aeppli, K. Lefmann, D. F. McMorrow, P. Worderwisch, P. Smeibidl, N. Mangkorntong, T. Sasagawa, M. Nohara, H. Takagi, and T. E. Mason, Nature (London) **415**, 299 (2002).
[90] S. Wakimoto, R. J. Birgeneau, Y. Fujimaki, N. Ichikawa, T. Kasuga, Y. J. Kim, K. M. Kojima, S.-H. Lee, H. Niko, J. M. Tranquada, S. Uchida, and M. v. Zimmerman, Phys. Rev. B **67**, 184419 (2003).
[91] X. J. Zhou, T. Yoshida, D.-H. Lee, W. L. Yang, V. Brouet, F. Zhou, W. X. Ti, J. W. Xiong, Z. X. Zhao, T. Sasagawa, T. Kakeshita, H. Eisaki, S. Uchida, A. Fujimori, Z. Hussain, and Z.-X. Shen, cond-mat/0403181 (unpublished).
[92] M. Granath, V. Oganesyan, D Orgad, and A. A. Kivelson, Phys. Rev. B **65**, 184501 (2002).
[93] M. Braden, W. Schnelle, W. Schwarz, N. Pyka, G. Heger, Z. Fisk, K. Gamayunov, I. Tanaka, and H. Kojima, Z. Phys. B: Condens. Matter **94**, 29 (1994).
[94] C.-H. Lee, K. Yamada, M. Arai, S. Wakimoto, S. Hosoya, and Y. Endoh, Physica C **257**, 264 (1996).
[95] H. Kimura, K. Hirota, C. H. Lee, K. Yamada, and G. Shirane, J. Phys. Soc. Jpn. **69**, 851 (2000).
[96] M. Nohara, T. Suzuki, Y. Maeno, T. Fujita, I. Tanaka, and H. Kojima, Phys. Rev. Lett. **70**, 3447 (1993).
[97] J. M. Tranquada, P. M. Gehring, G. Shirane, S. Shamoto, and M. Sato, Phys. Rev. B **46**, 5561 (1992).
[98] B. J. Sternlieb, J. M. Tranquada, G. Shirane, M. Sato, and S. Shamoto, Phys. Rev. B **50**, 12 915 (1994).
[99] P. Bourges, H. F. Fong, L. P. Regnault, J. Bossy, C. Vettier, D. L. Milius, I. A. Aksay, and B. Keimer, Phys. Rev. B **56**, R11 439 (1997).
[100] H. A. Mook, P. Dai, S. M. Hayden, G. Aeppli, T. G. Perring, and F. Doğan, Nature (London) **395**, 580 (1998).
[101] P. Dai, H. A. Mook, and F. Doğan, Phys. Rev. Lett. **80**, 1738 (1998).
[102] H. A. Mook, P. Dai, F. Doğan, and R. D. Hunt, Nature (London) **404**, 729 (2000).
[103] C. Stock, W. J. L. Buyers, R. Liang, D. Peets, Z. Tun, D. Bonn, W. N. Hardy, and R. J. Birgeneau, Phys. Rev. B **69**, 014502 (2004).
[104] H. A. Mook, P. Dai, and F. Doğan, Phys. Rev. Lett. **88**, 097004 (2002).
[105] P. Bourges, Y. Sidis, H. F. Fong, L. P. Regnault, J. Bossy, A. Ivanov, and B. Keimer, Science **288**, 1234 (2000).
[106] M. Ito, H. Harashina, Y. Yasui, M. Kanada, S. Iikubo, M. Sato, A. Kobayashi, and K. Kakurai, J. Phys. Soc. Jpn. **71**, 265 (2002).
[107] M. Arai, T. Nishijima, Y. Endoh, T. Egami, S. Tajima, K. Tomimoto, Y. Shiohara, M. Takahashi, A. Garrett, and S. M. Bennington, Phys. Rev. Lett. **83**, 608 (1999).
[108] D. Reznik, P. Bourges, L. Pintschovius, Y. Endoh, Y. Sidis, T. Matsui, and S. Tajima, cond-mat/0307591 (unpublished).
[109] S. M. Hayden, H. A. Mook, P. Dai, T. G. Perring, and F. Doğan (unpublished).
[110] P. Dai, H. A. Mook, R. D. Hunt, and F. Doğan, Phys. Rev. B **63**, 054525 (2001).
[111] D. Podolsky, E. Demler, K. Damle, and B. I. Halperin, Phys. Rev. B **67**, 094514 (2003).